Stress, birefringence, and conformational relaxation of an initially straight stiff bead-rod polymer

I. D. Dissanayake and P. Dimitrakopoulos
Department of Chemical and Biomolecular Engineering, University of Maryland, College Park, Maryland 20742, USA
(Received 16 May 2005; revised manuscript received 12 May 2006; published 22 August 2006)

The stress and optical relaxation of an initially straight stiff polymer chain are studied through Brownian dynamics simulations (based on a semiflexible bead-rod model) covering a broad range of time scales and polymer lengths. The strong stress component σ_{11} (where "1" is the direction of the original alignment) is shown to be associated with the chain's longitudinal relaxation while the weak stress component $\sigma_{22}=\sigma_{33}$ is shown to depend on the chain's transverse relaxation. The two independent stress components follow a different relaxation; this anisotropy is shown to result from the participation of the different relaxation modes in the transverse direction. The chain's optical relaxation is shown to be affected by the longitudinal dynamics only. The early relaxation of the strong stress component σ_{11} and that of the chain's optical properties constitute a universal behavior—i.e., valid for any stiffness of the bead-rod chain, since at the early times the bending forces do not affect the longitudinal dynamics. Based on the knowledge of the physical mechanism and the chain's conformational behavior, we predict and explain the polymer stress and optical relaxation. A nonlinear stress-optic law (valid for any time and chain stiffness) is derived based on the identified relation of the chain configuration with the optical properties and the polymer stress. A coarse-grain model describing extended semiflexible bead road chains is also derived.

DOI: 10.1103/PhysRevE.74.021918 PACS number(s): 87.15.−v, 83.80.Rs, 83.10.Mj, 89.75.Da

I. INTRODUCTION

The present study considers the relaxation of a single stiff polymer chain from an initial straight configuration in a viscous solvent. Physically this problem may correspond to the case of a polymer chain fully stretched by a strong flow and then relaxed by switching the flow off. This problem is also motivated by recent experiments with single biological molecules relaxing after being fully extended by applied forces as well as by the recent development of microdevices involving stretched tethered biopolymers (e.g., [1–3]). In this article, we focus our attention on the stress and birefringence relaxation and how they are affected by the corresponding configuration relaxation. Our interest lies on stiff polymers—i.e., polymers whose persistence length is larger than their contour length. Our results are applicable to both synthetic and biological stiff polymers such as Kevlar, polyesters, actin filaments, microtubules and rodlike viruses.

The study of the dynamics of semiflexible polymers has received much attention during the last years. The persistence length of individual molecules of these polymers varies from 50 nm for DNA to near 15 μm for F-actin and 10 mm for microtubules (e.g., see [4–6]). By considering that the smallest length associated with these biopolymers is the diameter of the individual molecule with a typical value of a few nanometers, we readily realize that semiflexible polymers show a broad range of stiffness which results in some unique properties of their solutions and networks. As a result, there has been recently a growing interest in understanding the properties of semiflexible polymers by both experimental and theoretical investigations.

Experimental studies employing macrorheological and microrheological approaches have considered the viscoelasticity of F-actin solutions and networks (e.g., [6–11]), microtubules [12], and synthetic polymers (e.g., [13–16]). Single-molecule probing techniques have allowed the investigation of the dynamics of DNA molecules (e.g., [1,2,17,18]) and stiffer biological polymers such as actin filaments (e.g., [19–21]) and microtubules (e.g., [12]). Theoretical investigations considered both the conformation and viscoelasticity of semiflexible polymer solutions especially near equilibrium (e.g., [22–28]). Studies of polymer solutions far from equilibrium include the problem of the chain being straightened by applied forces (e.g., [29,30]) as well as the dynamics of a chain under various external perturbations [31].

In this paper we study the stress and birefringence relaxation of an initially straight stiff polymer. A number of authors (e.g., [32–36]) have studied the corresponding problem for flexible polymers. A review has been given in our recent paper [37] where we investigated both the transverse and longitudinal dynamics for a flexible bead-rod chain and showed that the polymer relaxation at intermediate times results from a quasisteady equilibrium of the tension forces in the longitudinal direction; i.e., it is the longitudinal dynamics that controls the chain relaxation. In the present study we focus our attention on the effects of the chain stiffness. Although we explicitly consider the relaxation of a single polymer chain in a viscous solvent, our results should be valid even for concentrated polymer solutions and networks as long as the relaxation of interest occurs on length scales shorter than that characterizing the entanglements or crosslinks.

By employing scaling laws, we numerically determine the relaxation of the polymer stress and birefringence over extended time scales and polymer lengths. In particular, we study chains with polymer lengths up to $N=40\,000$ while by combining our results for the three time behaviors, we cover near 25 time decades. After discussing the mathematical formulation and the numerical algorithm in Sec. II, we present and analyze the stress relaxation in Sec. III. The chain's optical relaxation (i.e., the relaxation of the polymer birefringence and the associated index-of-refraction tensor) is considered in Sec. IV. In both sections, we employ the relaxation

mechanism and the configuration evolution we identified in our earlier study [38] to predict and explain the relaxation of the polymer stress and birefringence. We also provide a detailed analysis of the relaxation of the chain's different modes and how they affect the chain evolution.

The strong stress component σ_{11} is shown to be associated with the chain's longitudinal relaxation while the weak stress component σ_{22} is shown to depend on the chain's transverse relaxation. Because for an incompressible fluid only the stress difference $\sigma_{11}-\sigma_{22}$ is meaningful, our study shows that for the current problem the stress difference consists of two components: a dominant one resulting from the relaxation of the chain length and a weak one resulting from the relaxation of the chain width. The chain's optical relaxation is shown to be affected by the longitudinal dynamics only. Since the bending forces do not affect the longitudinal dynamics at early times, the early behavior of the strong stress component σ_{11} and that of the chain's optical properties are universal—i.e., valid for any chain stiffness.

In addition, by combining the relation between the optical properties and the chain configuration with the relation between the polymer stress and the chain conformational evolution, in Sec. V we propose a generalized stress-optic law describing the relaxation for any chain stiffness and time period. As discussed in Sec. VI, the inherent nonlinearity of the current problem, associated with the initial straightness of the polymer chain, results in a nonlinear force-extension relation and thus a nonlinear stress-optic law which obviously contradicts the common linear relationship [39,40]. A coarse-grain model describing extended semiflexible bead road chains (ESBRC) is also derived.

We emphasize that the numerical results and the physical insight presented in this paper are based on a bead-rod model described in the next section, and thus they should not be confused with those from other polymer models. The bead-rod model we employ in this study has the important physical feature of preserving the length at the local scale (and thus the contour length of the entire chain) at all times. In addition, note that our study investigates a problem of nonlinear dynamics (i.e., nonlinear perturbations far from equilibrium); thus our results should not be confused with those in the linear regime—e.g., [22,23,27,28]. Some additional issues involving our computational model and results and their association with recent analytical predictions are addressed in Sec. VII.

II. MATHEMATICAL FORMULATION AND COMPUTATIONAL ALGORITHM

A discretized version of the wormlike chain model [41,42] is employed based on a Brownian dynamics method developed in Ref. [32]. This method considers a (flexible) bead-rod model with fixed bond lengths and ignores hydrodynamic interactions among beads as well as excluded-volume effects. (For the extended stiff chains we study in this paper, hydrodynamics has little effect on intrachain dynamics [41].) The polymer chain is modeled as $N_B=(N+1)$ identical beads connected by N massless links of fixed length b (which is used as the length unit). The position of bead i is denoted as $\boldsymbol{X}_i$, while the link vectors are given by $\boldsymbol{d}_i=\boldsymbol{X}_{i+1}-\boldsymbol{X}_i$.

To account for polymer stiffness, we add a bending energy proportional to the square of the local curvature. For a continuous chain the bending energy is given by

$$\phi^{bend}=\frac{\mathcal{E}b}{2}\int_0^L\left(\frac{\partial\hat{\boldsymbol{d}}}{\partial s}\right)^2 ds=\frac{\mathcal{E}b}{2}\int_0^L\left(\frac{\partial^2\boldsymbol{X}}{\partial s^2}\right)^2 ds, \tag{1}$$

where L is the (constant) contour length of the chain and $\hat{\boldsymbol{d}}$ the local unit tangent. The bending energy $\mathcal{E}$ is related to the persistence length L_p via $\mathcal{E}/k_BT\equiv L_p/b$, where k_B is the Boltzmann constant. The bending energy of the discrete model is given by

$$\phi^{bend}=\frac{\mathcal{E}b}{2}\sum_{i=2}^{N}\left(\frac{\boldsymbol{X}_{i+1}-2\boldsymbol{X}_i+\boldsymbol{X}_{i-1}}{b^2}\right)^2 b=\mathcal{E}\sum_{i=1}^{N-1}\left(1-\frac{\boldsymbol{d}_i\cdot\boldsymbol{d}_{i+1}}{b^2}\right), \tag{2}$$

and thus it depends on the angle θ_i between two successive links since $\boldsymbol{d}_i\cdot\boldsymbol{d}_{i+1}=b^2\cos\theta_i$. The properties of the polymer chain are specified by the (constant) contour length of the chain L and its persistence length L_p or equivalently in dimensionless form by the number of links N and the dimensionless bending energy $E=\mathcal{E}/k_BT$.

Assuming that the bead inertia is negligible, the sum of all forces acting on each bead i must vanish, which leads to the following Langevin equation

$$\zeta\frac{d\boldsymbol{X}_i}{dt}=\boldsymbol{F}_i^{bend}+\boldsymbol{F}_i^{rand}+\boldsymbol{F}_i^{ten}+\boldsymbol{F}_i^{cor}, \tag{3}$$

where the friction coefficient ζ is assumed to be uniform. $\boldsymbol{F}_i^{rand}$ is the Brownian force due to the constant bombardments of the solvent molecules. The force $\boldsymbol{F}_i^{ten}=T_i\boldsymbol{d}_i-T_{i-1}\boldsymbol{d}_{i-1}$, where T_i is a constraining tension along the direction of each link $\boldsymbol{d}_i$, ensures the link inextensibility. $\boldsymbol{F}_i^{cor}$ is a corrective potential force added so that the equilibrium probability distribution of the chain configurations is Boltzmann. (More details on how to determine efficiently these forces may be found in Ref. [32].) The bending force $\boldsymbol{F}_i^{bend}$ is derived from the discrete form of the bending energy, Eq. (2),

$$\boldsymbol{F}_i^{bend}=-\frac{\partial\phi^{bend}}{\partial\boldsymbol{X}_i}=\frac{\mathcal{E}}{b^2}\sum_{j=i-2}^{i}\left[\delta_{j,i-2}\boldsymbol{d}_{i-2}+\delta_{j,i-1}(\boldsymbol{d}_i-\boldsymbol{d}_{i-1})-\delta_{j,i}\boldsymbol{d}_{i+1}\right]. \tag{4}$$

In the equation above as well as in all the equations in this paper, a term exists only if its index can be defined within its permitted bounds. For example, for $i=N$ the term $\boldsymbol{d}_{i+1}$ in Eq. (4) does not exist, while for $i=1$ only the term $\boldsymbol{d}_{i+1}$ exists. We note that, in deriving Eq. (4), we used the fact that the link lengths are fixed. The same modeling of the chain stiffness may also be employed for variable link lengths—e.g., for a bead-spring model; in this case the equation for the bending force contains some additional terms from the differentiation of the link lengths.

The resulting system based on Eq. (3) may be solved in $O(N)$ operations facilitating the study of long and stiff chains. Ensemble averages are determined by employing 10^4 to 10^5 independent initial configurations. The polymer stress $\boldsymbol{\sigma}=-\Sigma_{i=1}^{N_B}\boldsymbol{X}_i\boldsymbol{F}_i^{total}$, where $\boldsymbol{F}_i^{total}$ is the sum of all forces appearing on the right-hand side of Eq. (3), is calculated efficiently by eliminating the fluctuating terms of large magnitude which produce vanishing expectation values [32]. In the following sections we present the polymer stress in units of k_BT. We emphasize that the numerical method employed in this work has been used to study semiflexible polymers near and far from equilibrium—e.g., [23,28,38]—and will not be discussed further in the present paper.

The birefringence B is a sensitive measure of the average conformation of the polymer molecules. For light propagating along the "3" direction, the dimensionless birefringence is given by [33]

$$B=\sqrt{(n_{11}-n_{22})^2+4n_{12}^2}, \tag{5}$$

where $\boldsymbol{n}$ is the dimensionless index-of-refraction tensor:

$$\boldsymbol{n}=\sum_{i=1}^{N}\boldsymbol{d}_i\,\boldsymbol{d}_i. \tag{6}$$

Both birefringence and the index-of-refraction tensor have been nondimensionalized with

$$\frac{2\pi}{9}\frac{(n^2+2)^2}{n}(\alpha_{\parallel}-\alpha_{\perp}), \tag{7}$$

where n is the isotropic part of the index-of-refraction tensor while $\alpha_{\parallel}$ and $\alpha_{\perp}$ are the polarizabilities parallel and perpendicular to a link, respectively [33]. For a straight chain aligned along the "1" direction, the birefringence is $B=N$ while the three relevant components of the index-of-refraction tensor, called refraction components in this article, are $n_{11}=N$ and $n_{22}=n_{12}=0$.

Our algorithm has been parallelized by employing message passing interface (MPI) and thus it can be used on both shared- and distributed-memory multiprocessor computers such as the IBM pSeries 690 and Linux Superclusters provided by the National Center for Supercomputing Applications (NCSA) in Illinois. On both types of machines, the efficiency is almost 100% even for a high number of processors. Utilizing this optimized parallel algorithm, we routinely employ up to 320 of the fastest processors to study single chains with more than $N=40\,000$ beads as we show in this paper and thus we are able to identify the polymer behavior of long chains or at very small times. The numerical method employed in this work has been used to study semiflexible polymers near equilibrium [27] as well as the relaxation of initially straight flexible and stiff polymers [37,38,43], and will not be discussed further in the present paper.

Throughout this paper, we denote the longitudinal and transverse lengths of the chain as $R_{\parallel}$ and $R_{\perp}$, of the links as $d_{\parallel}$ and $d_{\perp}$, and the longitudinal and transverse positions of the beads (with respect to the chain's center of mass) as $X_{\parallel}$ and $X_{\perp}$, respectively. (The longitudinal and transverse directions refer to the orientation of the entire chain.) We emphasize that for an elongated chain, the chain's width $R_{\perp}$ scales similarly to the transverse bead position $X_{\perp}$, while the chain's length $R_{\parallel}$ scales similarly to the sum of the longitudinal length $d_{\parallel}$ of all links—i.e., $R_{\parallel}\sim\Sigma d_{\parallel}$. In addition, owing to the link inextensibility, the transverse length $d_{\perp}$ of a link is associated with its longitudinal length $d_{\parallel}$—i.e., $d_{\perp}^2=b^2-d_{\parallel}^2$, where b is the fixed distance between two successive beads. Thus, properties which depend on $R_{\parallel}$, $d_{\parallel}$, or $d_{\perp}$ should scale with the chain's length, while those which depend on $R_{\perp}$ or $X_{\perp}$ should scale with the chain's width.

The Brownian forces give rise to a microscopic time scale associated with the diffusive motion of one bead, $\tau_{rand}=\zeta b^2/k_BT$, which is used as the unit for the times reported in this work if no other unit is used. Similarly, the bending forces give rise to a microscopic time scale associated with the relaxation of the angle between two successive links. For large bending energy $E\gg 1$, this time scale is given by $\tau_{bend}=\zeta b^2/\mathcal{E}=\tau_{rand}/E\ll\tau_{rand}$. This time scale also constitutes the first of a series of time scales associated with the bending vibrations of portions of the polymer chain with increasing length. The largest time scale, associated with the entire polymer chain, is denoted as $\tau_{\perp}\sim\zeta L^4/\mathcal{E}b^2=(N^4/E)\tau_{rand}$.

All properties presented in this paper are calculated as, and refer to, the ensemble averages of the corresponding instantaneous values. The birefringence is formally calculated by Eq. (5). Owing to the fact that the refraction component n_{12} is always negligible for the current problem (as discussed in Sec. IV), the formal calculation of the birefringence is identical to the ensemble average of the instantaneous values of this quantity. In the figures presented in the next sections, the polymer length may be presented by either the number of beads N_B or the number of links N. Obviously for long enough chains there is no difference, but for small to moderate length chains the difference may be significant. Thus in the figures below we use that number which produces the best fitting in the scaling laws with the understanding that for long enough chains there is no distinction.

III. STRESS AND CONFORMATIONAL RELAXATION

Forcing a polymer chain to obtain a straight configuration, the polymer accumulates only normal stresses which decay as the chain relaxes towards the equilibrium shape. Assuming that "1" is the direction of the initial configuration, the strong component of the normal stress is σ_{11}, while the other two components are equal, $\sigma_{22}=\sigma_{33}$, owing to symmetry. Also no shear stress develops in our system (i.e., $\sigma ij=0$ for any $i\neq j$). At equilibrium the stress is simply $\boldsymbol{\sigma}=-\boldsymbol{I}$ (where $\boldsymbol{I}$ is the unit 3×3 matrix—e.g., $\sigma_{11}=\sigma_{22}=-1$) owing to the motion of the center of mass as discussed in our previous article on the relaxation of flexible chains [37]. Subtracting the equilibrium value, the two independent nonzero components of stress (σ_{11} and σ_{22}) have opposite signs since in the "1" direction the polymer chain is being compressed while in the other two directions the chain is being extended. (Based on the way we define the stress, $\sigma_{11}+1>0$ while $\sigma_{22}+1<0$.) Thus in the figures below we plot the strong component as $(\sigma_{11}+1)$, and the weak component as $-(\sigma_{22}+1)$.

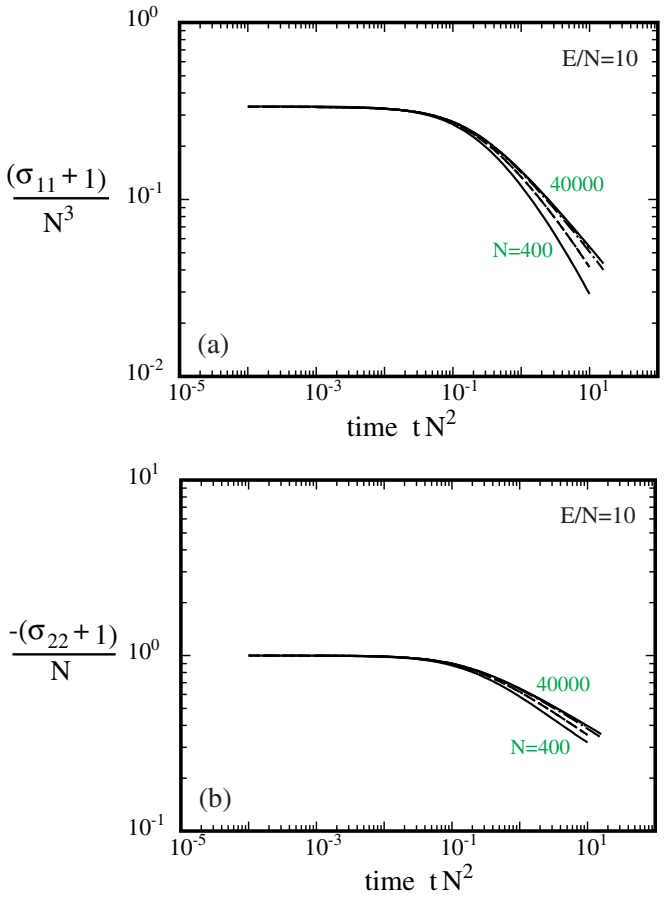

FIG. 1. (Color online) Stress relaxation of a long stiff polymer chain with $E/N=10$ at short times. Scaling law for the stress components (a) $(\sigma_{11}+1)$ and (b) $(\sigma_{22}+1)$. [Note that $(\sigma_{22}+1)$ is negative.] Both curves were generated by employing chains with $N=400, 1000, 4000, 10000, 40000$.

A. Short times

Considering a straight polymer chain, the bending forces are exactly zero and thus they do not affect the initial polymer stress. Therefore, for this problem a stiff chain is expected to show an initial stress identical to that of a flexible chain. The strong-stress component scales as $\sigma_{11}\sim N^3$ associated with $O(N^2)$ link tensions (necessary to maintain link inextensibility) for each of the N links [32]. On the other hand, the weak-stress component is exactly $\sigma_{22}=-(N+1)$ associated with the transverse component of the Brownian forces—i.e., $O(1)$ stresses per bead over $(N+1)$ beads [37]. Therefore, even dilute polymer solutions of stiff chains under strong extensional flows are expected to show large stresses associated with the strong stress component σ_{11}.

To verify our conclusions above and in addition to determining the time scale of the initial stress relaxation, in Fig. 1 we plot the polymer stress just after the chain is left to relax for long stiff chains with $E/N=10$. As this figure reveals, initially $\sigma_{11}=O(N^3)$ while $\sigma_{22}=-(N+1)$. In addition, the initial decay from the plateau occurs at times $t\sim\tau_{ten}\sim N^{-2}$ for both stress components.

Figure 1 reveals that the initial stress relaxation of long stiff chains is identical to that of flexible chains [37], and thus it can be explained similarly. In particular the short-time behavior of all chains denotes a period of dominant transverse motion; each polymer bead shows a transverse free diffusion $X_\perp\sim R_\perp\sim t^{1/2}$ due to the dominant effective Brownian force $F_\perp^{rand}\sim t^{-1/2}$. Owing to the link inextensibility, the longitudinal length of each link is shortened as $b^2-d_\parallel^2=d_\perp^2\sim t$ which results in a chain's length reduction $R_\parallel^2(0)-R_\parallel^2\sim N^2b^2-N^2d_\parallel^2\sim N^2t$ [38]. The dominant force in the longitudinal direction is the corresponding component of the tension force $F_\parallel^{ten}\sim Td_\parallel\sim N^2$ (since $T\sim N^2$ are the tensions along the nearly straight chain).

We emphasize that during the short times, the dominant forces in the longitudinal and transverse directions are not able to produce any stress relaxation: $\sigma_{11}\sim\Sigma Td_\parallel^2\sim NT\sim N^3$—i.e., it results from $O(N^2)$ link tensions for each of the N links—while $\sigma_{22}\sim\Sigma X_\perp F_\perp\sim N$—i.e., it is associated with the transverse Brownian forces.

The transition from short to intermediate times occurs when one of two dominated transverse forces $F_\perp^{ten}\sim Td_\perp\sim N^2t^{1/2}$ and $F_\perp^{bend}\sim Ed_\perp\sim Et^{1/2}$ balances the transverse Brownian force $F_\perp^{rand}$. For long enough stiff chains—i.e., for $N\geq(E/N)$—$F_\perp^{ten}$ balances first $F_\perp^{rand}$ at times $\tau_{ten}\sim N^2$ which thus denote the end of the short-time behavior as clearly shown in Fig. 1 above.

Short stiff chains are expected to show a behavior similar to that of long chains during short times. To verify this, we determined the stress and configuration evolution for short stiff chains with $N\leq100$ and the same stiffness ratio $E/N=10$. As shown in Fig. 2, the two independent stress components are again $\sigma_{11}\sim N^3$ and $\sigma_{22}=-(N+1)$.

The difference between long and short stiff chains lies on the time scale denoting the end of the short-time behavior. As Fig. 2 clearly shows, for short chains the transition to the intermediate-time behavior occurs at times $t\sim\tau_{bend}\sim E^{-1}$. The explanation for this difference lies in the fact that for short enough stiff chains, the transverse bending force grows faster than the transverse tension force during the short times, and thus it balances first the transverse Brownian force at times τ_{bend} (i.e., requiring that $F_\perp^{bend}\leq F_\perp^{rand}$ result in $t\leq\tau_{bend}$). The distinction between short and long stiff chains can be easily made by requiring that $F_\perp^{bend}\geq F_\perp^{ten}$ or equivalently $\tau_{bend}\leq\tau_{ten}$ which results in $N\leq(E/N)$. We can also obtain a more accurate description if we include the numerical coefficient of the two time scales. Figure 2 shows that $\tau_{bend}\approx10^{-3}E^{-1}$ while Fig. 1 shows that $\tau_{ten}\approx10^{-2}N^{-2}$, and thus the requirement $\tau_{bend}\leq\tau_{ten}$ is valid for $N\leq10(E/N)$. For chains with stiffness ratio $E/N=10$, the polymer length should be $N\leq100$, in agreement with our numerical results shown in Fig. 2 above.

As a conclusion, during the short times the dominant transverse Brownian force $F_\perp^{rand}\sim t^{-1/2}$ on each polymer bead produces a transverse free diffusion $R_\perp^2\sim t$ and a (constant) weak stress component $\sigma_{22}=-(N+1)$. Owing to the link inextensibility, the width increase results in a length reduction $R_\parallel^2(0)-R_\parallel^2\sim N^2t$. The dominant longitudinal tension force $F_\parallel^{ten}\sim N^2$ produces a (constant) strong stress component $\sigma_{11}\sim N^3$. The end of the short-time behavior occurs when the transverse tension or bending force on each bead balances the transverse Brownian force; this happens at times τ_{ten}

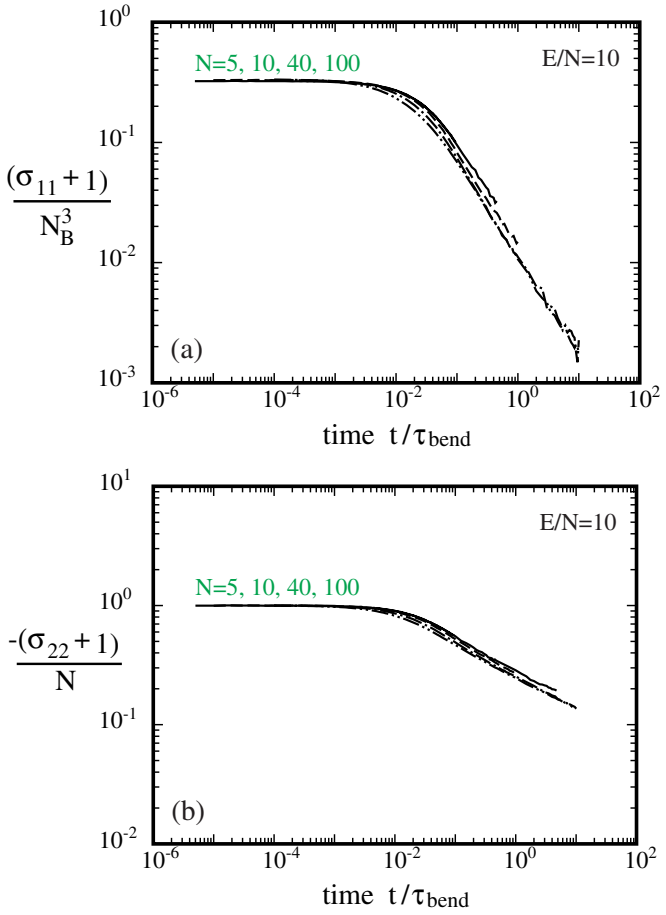

FIG. 2. (Color online) Stress relaxation of a short stiff polymer chain with $E/N=10$ at short times. Scaling law for the stress components (a) $(\sigma_{11}+1)$ and (b) $(\sigma_{22}+1)$. Both curves were generated by employing chains with $N=5,10,40,100$.

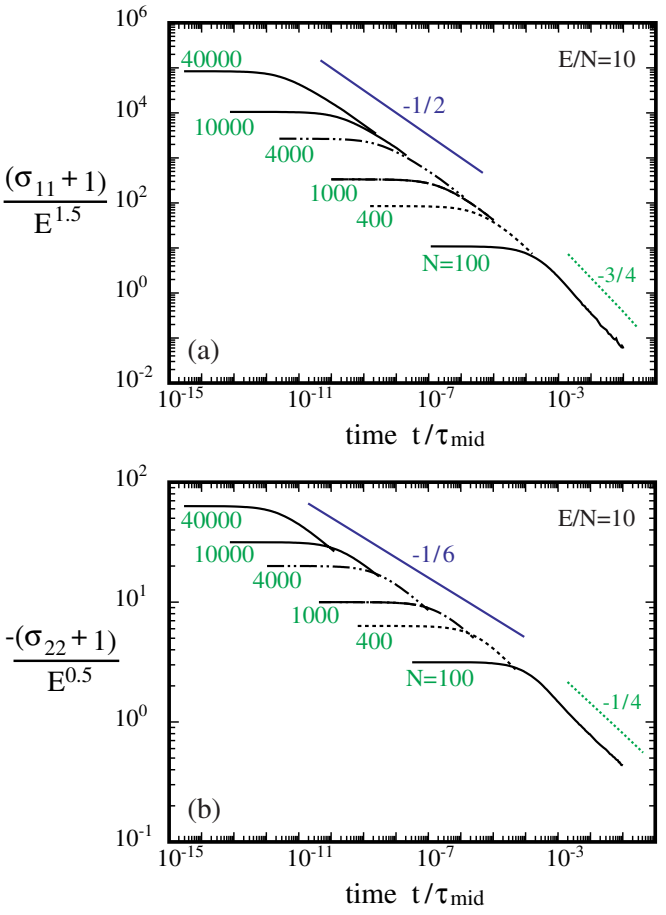

FIG. 3. (Color online) Stress relaxation of a stiff polymer chain with $E/N=10$ at early intermediate times. Scaling law for the stress components (a) σ_{11} and (b) σ_{22}. The curves were generated by employing chains with $N=400,1000,4000,10000,40000$. Also shown is the power-law decay at late intermediate times.

$\sim N^{-2}$ for long stiff chains $N \geq (E/N)$ and at times $\tau_{bend} \sim E^{-1}$ for short stiff chains $N \leq (E/N)$. Thus, short times denote a period of dominant transverse motion for the polymer chain which is not able to induce any stress relaxation.

B. Early intermediate times

At the end of the short times, the transverse free diffusion of the polymer beads is arrested; during the intermediate times all the length scales of the chain affect the polymer relaxation and a (significant) relaxation of the accumulated $O(N^2)$ tensions and $O(N^3)$ stresses is expected. As we discussed in Ref. [38], the intermediate times for stiff chains are divided into two physically different periods. During the early intermediate times, the longitudinal bending force $F_{\parallel}^{bend}$ is negligible compared to the strong tension force $F_{\parallel}^{ten} = O(N^2)$. (We recall that for a straight stiff chain, $F_{\parallel}^{bend}$ is identically zero.) Thus the early relaxation is identical to that for flexible chains. On the other hand, the bending forces affect the late period of the relaxation, until the end of the bending relaxation at times $\tau_{\perp} \sim N^4/E$. The transition times between the two periods has been identified in our previous work as the times $\tau_{mid} \sim N^4/E^3$ [38].

The stress relaxation at early intermediate times $\tau_{ten} \ll t \ll \tau_{mid}$ is shown in Fig. 3, where a power-law decay is clearly evident over eight time decades. We note that we produce this behavior by employing the scaling-law methodology—i.e., by monitoring the polymer stress of chains with increasing length over a short time period only, while in the corresponding figure the time and stresses are scaled with their values at the end of the behavior. (More details may be found in our earlier publication [43].) Figure 3 shows that at early intermediate times the polymer stress is

$$\frac{\sigma_{11}}{E^{1.5}} \sim \left(\frac{t}{N^4 E^{-3}}\right)^{-1/2} \quad \text{or} \quad \sigma_{11} \sim N^2 t^{-1/2}, \tag{8}$$

$$\frac{\sigma_{22}}{E^{0.5}} \sim \left(\frac{t}{N^4 E^{-3}}\right)^{-1/6} \quad \text{or} \quad \sigma_{22} \sim N^{2/3} t^{-1/6}. \tag{9}$$

Thus an anisotropy in the stress relaxation is observed at early intermediate times. Comparing these results to those for flexible chains, we observe that the strong-stress component σ_{11} shows exactly the same relaxation for both chains—i.e., its behavior is universal for any stiffness of the bead-rod

chain. On the other hand, the weak stress component of flexible chains shows a slower relaxation, $(\sigma_{22})_{\text{flex}} \sim N^{1/2} t^{-1/4}$ [37].

We emphasize that all power laws presented in this paper via our computational results can be verified through simple scaling arguments. For example, as discussed in the next section, the relaxation of the strong-stress component during the late intermediate times, is $\sigma_{11} \sim N^3 E^{-3/4} t^{-3/4}$. (Note that this law is derived from the relaxation of short stiff chains in the entire intermediate times and thus is independent of the early intermediate-time behavior of long stiff chains presented in this section.) Thus during the early intermediate times, the strong-stress component decreases from a magnitude of $\sigma_{11} = O(N^3)$ at short times $\tau_{ten} \sim N^{-2}$ to a magnitude of $\sigma_{11} = O(E^{3/2})$ at the transition times $\tau_{mid} \sim N^4/E^3$. Matching these two stresses with a single power law t^a gives

$$(\sigma_{11})_{short} \sim N^3 \left(\frac{t}{N^{-2}} \right)^a \sim (\sigma_{11})_{late} \sim E^{3/2} \left(\frac{t}{N^4 E^{-3}} \right)^a, \tag{10}$$

which is only valid for $a = -1/2$ and thus at early intermediate times $\sigma_{11} \sim N^2 t^{-1/2}$ in agreement with our numerical results shown in Fig. 3(a). The same can easily be shown for the weak-stress component σ_{22}.

To explain the relaxation of the two independent stress components we utilize the configuration relaxation mechanism we have identified in our previous study [38]. In particular, during the early intermediate times there is a quasi-steady equilibrium of tensions associated with the deforming action of the Brownian forces, $T \sim N t^{-1/2}$. During these times the polymer length decreases as $R_\parallel^2(0) - R_\parallel^2 \sim N t^{1/2}$ or $\Delta R_\parallel = R_\parallel(0) - R_\parallel \sim t^{1/2}$ while the chain width increases as $R_\perp^2 \sim N^{-1/3} t^{5/6}$ [38].

Based on the mechanism above, it is straightforward to show that the relaxation of the strong-stress component σ_{11} is associated with the longitudinal dynamics only. In particular, by considering the entire polymer chain or summing over all beads, we obtain

$$\sigma_{11} \sim R_\parallel F_\parallel \sim N d_\parallel F_\parallel \sim N^2 t^{-1/2}, \tag{11}$$

where we use that $d_\parallel \sim 1$, $R_\parallel \sim N$, and $F_\parallel \sim T d_\parallel \sim T$. On the other hand, we may conclude that the relaxation of the weak-stress component σ_{22} results from the relaxation of the polymer width only. In particular, the transverse evolution of the polymer chain, $R_\perp \sim X_\perp \sim N^{-1/6} t^{5/12}$, reveals the dominant transverse force on each bead:

$$F_\perp \sim \zeta \frac{dX_\perp}{dt} \sim N^{-1/6} t^{-7/12}. \tag{12}$$

Thus by summing over all beads, the stress decay is

$$\sigma_{22} \sim N X_\perp F_\perp \sim N^{2/3} t^{-1/6}, \tag{13}$$

in agreement with our numerical results shown in Fig. 3(b).

The anisotropy in the polymer relaxation depicted at Eqs. (8) and (9) above may be attributed to the participation of the different relaxation modes in the transverse direction. In particular, note that if the chain were to relax transversely with only the shortest mode, the width evolution would be $(R_\perp^2)_{SM} \sim d_\perp^2 \sim b^2 - d_\parallel^2$ or

$$(R_\perp^2)_{SM} \sim N^{-2} [R_\parallel^2(0) - R_\parallel^2] \sim N^{-1} t^{1/2}, \tag{14}$$

which obviously underestimates the true width evolution. On the other hand, if the chain were to relax transversely with only the longest mode, then the width evolution would be

$$(R_\perp^2)_{LM} \sim R_\parallel^2(0) - R_\parallel^2 \sim N t^{1/2}, \tag{15}$$

which overestimates the true width evolution. The participation of the different modes in the transverse relaxation results in a relaxation rate between the two extreme rates of the shortest and longest modes. In addition, we note that if the chain were to relax transversely with only one relaxation mode, then the width growth $R_\perp^2$ should follow the same power law as the length reduction $R_\parallel^2(0) - R_\parallel^2$—i.e., a $t^{1/2}$ power law as the growths of the shortest and longest mode verify; thus the anisotropic relaxation results from the participation of the different relaxation modes in the chain's transverse evolution.

Proceeding further, we may conclude that at the beginning of the intermediate times $t \sim N^{-2}$ the chain relaxes transversely with its smallest mode only owing to the short-time transverse free diffusion (i.e., $R_\perp^2 \sim d_\perp^2$) while as the time increases longer modes participate in the chain relaxation. To provide a qualitative picture of the mode relaxation, we may determine the evolution of the average relaxation mode by replacing the contribution of the different modes by a single mode with a time-dependent length and amplitude. The transverse growth of such mode is the same as that for the entire chain—i.e., $R_\perp$—while the link inextensibility at the mode wave results in a time-dependent wave number N_M which should follow the requirement $R_\perp^2 \sim N_M^{-2} [R_\parallel^2(0) - R_\parallel^2]$ and thus

$$N_M \sim N^{2/3} t^{-1/6}. \tag{16}$$

Therefore, the wave number of the average mode decreases with time, from $N_M \sim N$ at times $\tau_{ten} \sim N^{-2}$, to $N_M \sim E^{1/2}$ at times $\tau_{mid} \sim N^4/E^3$; i.e., the mode's wavelength increases with time from $R_\parallel^M \sim 1$ at τ_{ten} to $R_\parallel^M \sim N/E^{1/2}$ at τ_{mid}.

The mechanism of the longitudinal relaxation of stiff chains is identical to that for flexible chains, and thus all polymer properties which depend on the chain longitudinal reduction should show a *universal* behavior—e.g., the strong-stress component σ_{11}. On the other hand, the chain's transverse evolution is affected by the chain stiffness and thus polymer properties which depend on the chain width do not show a universal behavior. To explain this, observe that, compared to a flexible chain, a stiff chain is less likely to relax transversely with short modes and thus for a given length reduction $R_\parallel^2(0) - R_\parallel^2$ the stiff chain shows a greater width evolution, $(R_\perp^2)_{\text{stiff}} \sim N^{-1/3} t^{5/6} \geq (R_\perp^2)_{\text{flex}} \sim N^{-1/2} t^{3/4}$. This results in a larger weak-stress component for the stiff chain, $(\sigma_{22})_{\text{stiff}} \sim N^{2/3} t^{-1/6} \geq (\sigma_{22})_{\text{flex}} \sim N^{1/2} t^{-1/4}$.

The different magnitudes of the two stress components at the end of the early intermediate times—i.e., $\sigma_{11} = O(E^{3/2})$ while $\sigma_{22} = O(E^{1/2})$—show that during the entire early inter-

mediate times the polymer chain is still far from equilibrium. This conclusion is also supported by the fact that even at times τ_{mid} the chain width is much smaller than its value near equilibrium—i.e., $(R_\perp^2)_{\text{mid}}=O(N^3/E^{5/2})\ll(R_\perp^2)_{\text{eq}}=O(N^3/E)$. We also conclude that the anisotropy in the stress relaxation is caused by the corresponding anisotropy in the configuration relaxation and thus by the influence of the different relaxation modes in the chain's transverse evolution.

C. Late intermediate times

We now turn our attention to the chain relaxation during the late intermediate times where the bending forces affect the longitudinal relaxation of the polymer chain. To reveal the polymer behavior during the times $\tau_{mid}\ll t\ll\tau_\perp$, ideally we would monitor a long chain over the extended period $[\tau_{ten},\tau_\perp]$ which is still computationally impractical to achieve. Clearly a scaling law should be used; in this case we should employ the property of the scaling law methodology which dictates that the behavior of short chains represents the late behavior of longer chains—i.e., property (iii) in Ref. [43]. For example, for stiff chains with $E/N=10$, we may expect to be able to capture the late intermediate-time behavior by employing chains with $N\leq 100$ (since we captured the early behavior with chains $100<N\leq 40\,000$ in Sec. III B.) It is important to realize that these short chains should show only one intermediate behavior over the entire period $\tau_{bend}\ll t\ll\tau_\perp$, identical to the late intermediate-time behavior of the long chains we seek. To explain this, observe that by requiring $\tau_{ten}\geq\tau_{mid}$ results in $N\leq(E/N)$; these short chains also show $\tau_{ten}\geq\tau_{bend}$. Therefore the two time scales of the early intermediate-time behavior, τ_{ten} and τ_{mid}, should disappear now. (Note that the first inequality shows that τ_{mid} disappears while the second one shows that τ_{ten} is replaced by τ_{bend} as the beginning of the intermediate times.) Combining this with the analysis for the short-time behavior presented earlier in Sec. III A, we may conclude that for short chains with $N\leq(E/N)$, after balancing the transverse Brownian forces at times $t\sim\tau_{bend}$, the bending forces start to affect both the transverse and the longitudinal relaxation of the polymer chain until the end of the bending relaxation at times $t\sim\tau_\perp$.

Figure 4 shows that during the late intermediate times the polymer stress is

$$\sigma_{11}\sim N^3E^{-3/4}t^{-3/4}\quad\text{and}\quad\sigma_{22}\sim NE^{-1/4}t^{-1/4}. \tag{17}$$

The (direct) dependence of both stress components on the chain stiffness E is in agreement with our conclusion that during these times the bending forces should affect the chain dynamics. The different power-law decays of the two stress components reveal that there exists an anisotropy in the stress relaxation even during the late intermediate times.

To explain the relaxation of the two independent stress components we utilize again the configuration relaxation mechanism we have identified in our previous study [38]. In particular, during the late intermediate times the polymer length reduction $R_\parallel^2(0)-R_\parallel^2\sim N^2E^{-3/4}t^{1/4}$ is associated with a $T\sim N^2E^{-3/4}t^{-3/4}$ relaxation of tensions affected by both

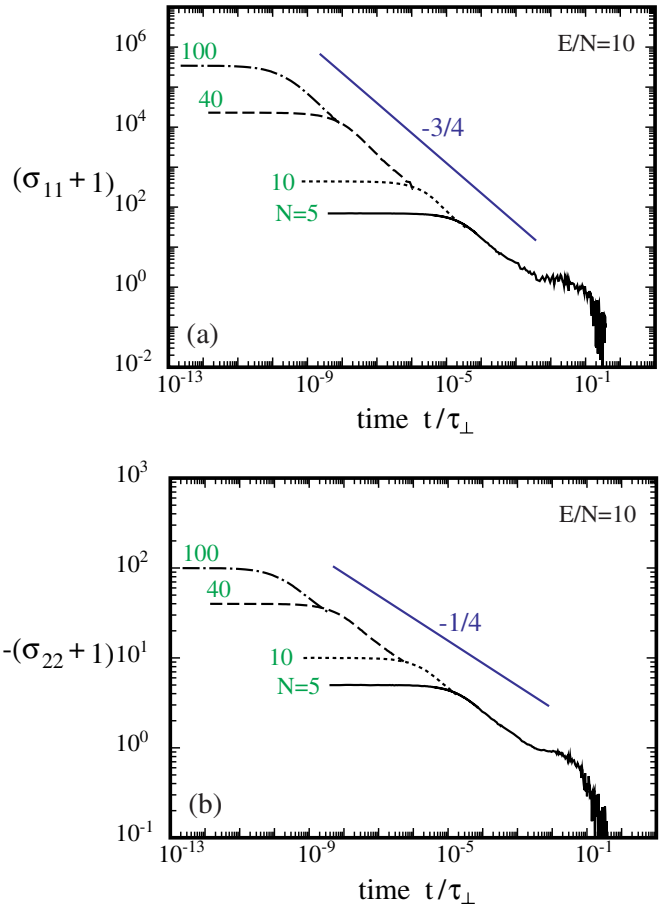

FIG. 4. (Color online) Stress relaxation of a stiff polymer chain with $E/N=10$ at late intermediate times: scaling law for the stress components (a) σ_{11} and (b) σ_{22}. The curves were generated by employing chains with $N=5,10,40,100$.

Brownian and bending forces. During the same times the chain width increases as $R_\perp^2\sim E^{-1/4}t^{3/4}$.

Similarly to our analysis for the early intermediate times, it is straightforward to show that the relaxation of the strong stress component σ_{11} is associated with the chain's longitudinal dynamics only. By considering the entire polymer chain or summing over all beads, we obtain

$$\sigma_{11}\sim R_\parallel F_\parallel\sim Nd_\parallel F_\parallel\sim N^3E^{-3/4}t^{-3/4}, \tag{18}$$

where we use that $d_\parallel\sim 1$, $R_\parallel\sim N$, and $F_\parallel\sim Td_\parallel\sim T$. The relaxation of the weak-stress component σ_{22} results from the relaxation of the polymer width only. In particular, the transverse evolution of the polymer chain, $R_\perp\sim X_\perp\sim E^{-1/8}t^{3/8}$, reveals the dominant transverse force on each bead,

$$F_\perp\sim\zeta\frac{dX_\perp}{dt}\sim E^{-1/8}t^{-5/8}, \tag{19}$$

and thus by summing over all beads, the stress decay is

$$\sigma_{22}\sim NX_\perp F_\perp\sim NE^{-1/4}t^{-1/4}, \tag{20}$$

in agreement with our numerical results shown in Fig. 4(b).

The anisotropy in the stress relaxation depicted at Eq. (17) above results from the participation of the different relax-

ation modes in the transverse direction, similar to what happens during the early behavior. To provide a qualitative picture of the mode relaxation, we determine again the evolution of the average relaxation mode by replacing the contribution of the different modes by a single mode with a time-dependent length and amplitude. The wave number N_M of this mode is given by $R_\perp^2 \sim N_M^{-2}[R_\parallel^2(0) - R_\parallel^2]$ or

$$N_M \sim NE^{-1/4}t^{-1/4}, \tag{21}$$

and thus it decreases with time from $N_M \sim E^{1/2}$ at times $\tau_{mid} \sim N^4/E^3$ to $N_M \sim 1$ at times $\tau_\perp \sim N^4/E$; i.e., the mode's wavelength increases with time from $R_\parallel^M \sim N/E^{1/2}$ at τ_{mid} to $R_\parallel^M \sim N$ at $\tau_\perp$. This means that at the end of the bending relaxation at times $\tau_\perp$, the polymer chain relaxes with its longest mode only as we can easily verify since at times $\tau_\perp$, $R_\perp^2 \sim R_\parallel^2(0) - R_\parallel^2 \sim N^3/E$.

As a conclusion, during the late intermediate times the chain longitudinal relaxation is associated with the relaxation of the dominant tensions which are now affected by both Brownian and bending forces. The tension relaxation $T \sim N^2E^{-3/4}t^{-3/4}$ is associated with a length reduction $R_\parallel^2(0) - R_\parallel^2 \sim N^2E^{-3/4}t^{1/4}$ and results in a strong-stress component relaxation of $\sigma_{11} \sim N^3E^{-3/4}t^{-3/4}$. Owing to the participation of the different relaxation modes in the transverse relaxation, the chain width increases anisotropically as $R_\perp^2 \sim E^{-1/4}t^{3/4}$; the dominant transverse force is $F_\perp \sim E^{-1/8}t^{-5/8}$ and the associated weak-stress component relaxes as $\sigma_{22} \sim NE^{-1/4}t^{-1/4}$. Therefore, the anisotropy in the stress relaxation is caused by the corresponding anisotropy in the configuration relaxation and thus by the influence of the different relaxation modes in the chain's transverse evolution.

The late intermediate-time behavior discussed in this section is valid for any stiff chain $E \geq N$. To verify this conclusion we determined the stress relaxation of a very stiff chain with $E/N=10^4$ at late intermediate times. As shown in Fig. 5, both stress components σ_{11} and σ_{22} of this chain show a behavior identical to that for a chain with $E/N=10$. Observe that for $E/N=10^4$ the late intermediate-time behavior is valid for smaller times (and longer chains) compared to that for $E/N=10$; to show this in this figure we include chains with $N=400,1000$ for the very stiff chain with $E/N=10^4$. We note that, in this figure, to distinguish the curves for the two chains we scale the time with $\tau_{rod} \sim N^3$—i.e., the long-time scale of the linear relaxation of stiff chains; if we scale the time with $\tau_\perp \sim N^3/E$, both curves fall as the one shown in Fig. 4 above.

The different magnitudes of the two stress components during the late intermediate times along with their anisotropic relaxation show that during these times the polymer chain is still far from equilibrium. Only at the end of the late intermediate behavior at times $\tau_\perp$ the chain is near equilibrium since then the two stress components have equal magnitudes, $\sigma_{11}=O(1)=\sigma_{22}$, while the chain width has reached its scale at equilibrium $(R_\perp^2)_{eq} \sim N^3/E$. (This fact results in an increased noise at the end of the curves in Figs. 4 and 5.)

Thus no long-time relaxation is present for the transient dynamics of stiff chains, in direct contrast to the flexible chains where a long-time exponential relaxation is necessary

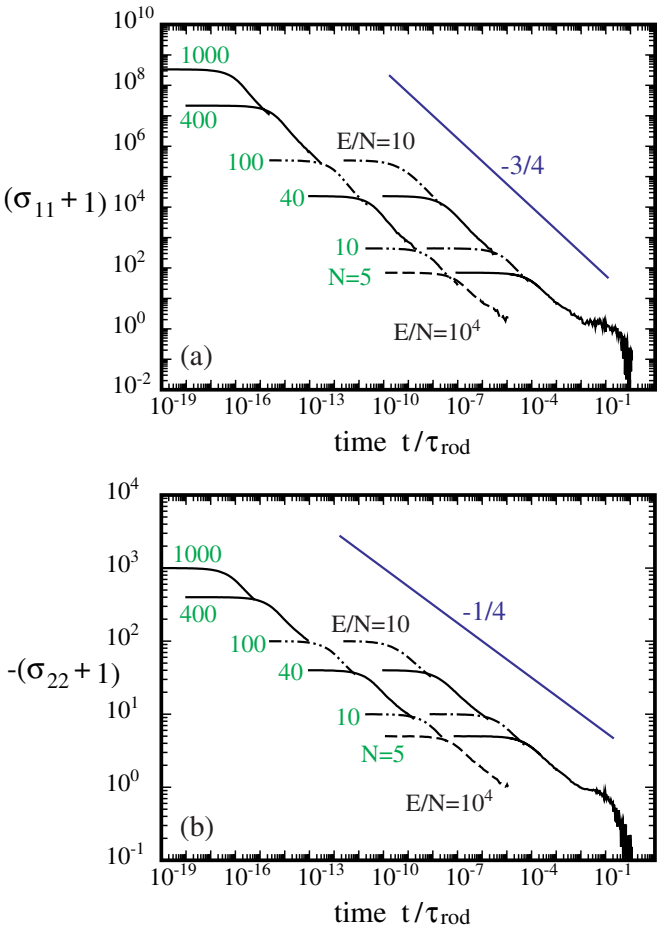

FIG. 5. (Color online) Stress relaxation of a stiff chain with $E/N=10$ and a very stiff chain with $E/N=10^4$ at late intermediate times: scaling laws for the stress components (a) σ_{11} and (b) σ_{22}. The curves were generated by employing chains with $N=5,10,40,100$ for $E/N=10$ and $N=5,10,40,100,400,1000$ for $E/N=10^4$. By scaling the time with $\tau_\perp$ instead of τ_{rod}, the curves for the two values of stiffness ratio E/N fall as the one shown in Fig. 4.

to revert the chain for a practically straight shape at the end of intermediate times to the equilibrium coil-like one (as we discussed in Ref. [37]). We emphasize that the final linear relaxation towards equilibrium (e.g., see [26–28]) is indistinguishable from the noise of the Brownian motion, and thus it cannot be revealed via transient Brownian dynamics (especially when no variance reduction technique is employed as happens in our study).

IV. BIREFRINGENCE RELAXATION

The relaxation of the birefringence for initially straight flexible chains was studied by Doyle, Shaqfeh, and Gast [33], where it was found that initially the birefringence decays linearly with time while for long times there is an exponential decay. In a subsequent study, Doyle *et al.* [34] studied the stress and birefringence relaxation of flexible chains following extensional flow. In the recent work of Ghosh *et al.* [44], a nonlinear relation between stress and

birefringence was proposed based on the similarities of the finitely extensible nonlinear elastic (FENE) and bead-rod models for extended flexible chains.

To be able to identify the optical relaxation at all times and, most importantly, to relate this relaxation to the configuration relaxation and the problem mechanism, we studied separately the relaxation of each of the three refraction components appearing in Eq. (5). The study of these components reveals that the contribution to birefringence of the component n_{12} is always negligible. (This component is at least two to three orders of magnitude smaller than the polymer birefringence.) Thus for the current problem Eq. (5) simplifies to

$$B \approx n_{11} - n_{22}. \tag{22}$$

Therefore, from now on, we focus our attention only on the relaxation of the refraction components n_{11} and n_{22}.

The first step in our analysis is to identify how exactly the chain's optical properties are associated with the chain configuration. We note that the refraction component n_{11} is directly associated with the longitudinal length of each link, $d_\parallel$, and thus with the chain's length $R_\parallel$,

$$n_{11} = \sum d_\parallel d_\parallel \sim N d_\parallel^2 \sim \frac{1}{N} R_\parallel^2. \tag{23}$$

The same happens for the refraction component n_{22}, which is directly related to the width of each link $d_\perp$,

$$n_{22} = \sum d_\perp d_\perp \sim N(b^2 - d_\parallel^2) \sim \frac{1}{N}[R_\parallel^2(0) - R_\parallel^2] \tag{24}$$

(i.e., owing to the link inextensibility, $d_\perp$ is associated with the link length $d_\parallel$ and thus with the chain's length). Thus, both refraction components are associated with the chain's length $R_\parallel$. The same is valid for birefringence owning to Eq. (22).

Therefore, the optical properties of initially extended polymers can be predicted and explained through the chain's longitudinal relaxation we have identified in our earlier study [38]. Our predictions are in excellent agreement with our numerical results at all times and polymer stiffness. To show this agreement, we present below our numerical results during intermediate times only due to the particular importance of this time period being affected by all the chain length scales.

During the short times $t \ll N^{-2}$ for all chains, the birefringence shows a linear dependence on time,

$$B(0) - B \sim \frac{1}{N}[R_\parallel^2(0) - R_\parallel^2] \sim Nt, \tag{25}$$

due to the corresponding free diffusion of the polymer beads [38]. Figure 6(a) reveals that during the early intermediate times of stiff chains, $\tau_{ten} \ll t \ll \tau_{mid}$, the polymer birefringence shows the expected $t^{1/2}$ power-law reduction,

$$B(0) - B \sim \frac{1}{N}[R_\parallel^2(0) - R_\parallel^2] \sim t^{1/2}. \tag{26}$$

[We emphasize that, in order to reveal the birefringence relaxation during the intermediate times, we should plot the birefringence reduction $B(0)-B$, and not the birefringence itself.] In addition, Fig. 6(b) shows that during the late intermediate times $\tau_{mid} \ll t \ll \tau_\perp$, the birefringence reduction is

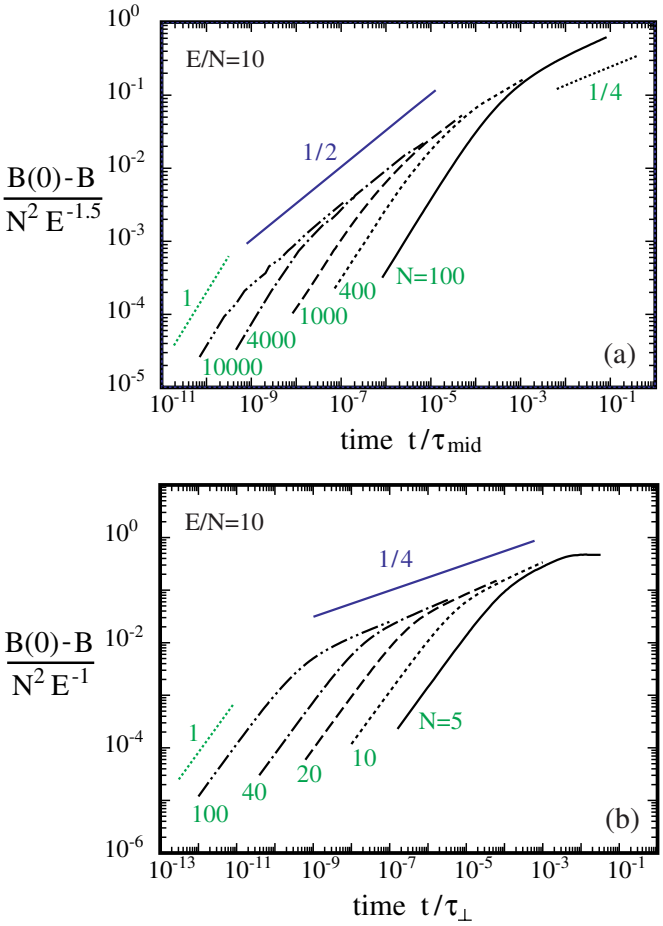

FIG. 6. (Color online) Scaling law for the birefringence relaxation at (a) early and (b) late intermediate times for a stiff chain with $E/N=10$. Also shown is the linear relaxation at short times.

$$B(0) - B \sim \frac{1}{N}[R_\parallel^2(0) - R_\parallel^2] \sim NE^{-3/4}t^{1/4}, \tag{27}$$

which is again in excellent agreement with our predictions based on the relation between the chain's optical properties and the polymer length.

We note that the birefringence relaxation shown in Fig. 6(a) constitutes a *universal* behavior valid for any polymer stiffness. To show this numerically, in Fig. 7 we present the same behavior during the intermediate times of flexible chains, $\tau_{ten} \ll t \ll \tau_{rouse}$ (where $\tau_{rouse} \sim N^2$).

As a closure to this section, we emphasize again that both refraction components n_{11} and n_{22} contribute significantly to the polymer birefringence at all times and for any chain stiffness. [This is supported by Eqs. (23) and (24) above as well as by direct comparison of our numerical results for the two refraction components, n_{11} and n_{22}.] Therefore in the study of optical properties the contribution of the refraction component n_{22} should not be discounted.

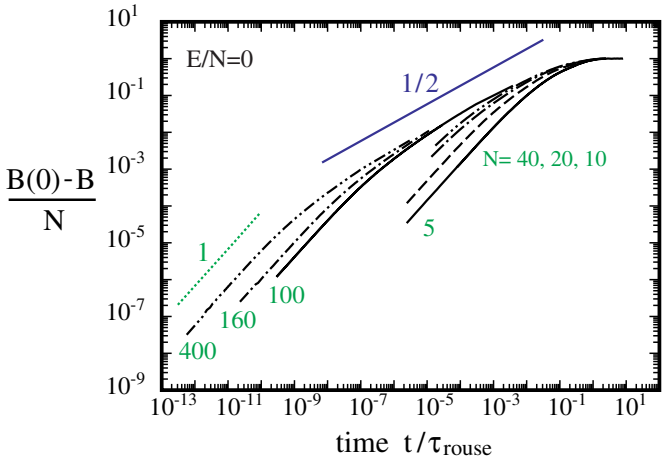

FIG. 7. (Color online) Scaling law for the birefringence relaxation at intermediate times for a completely flexible chain ($E=0$). Also shown is the free diffusion at short times.

V. GENERALIZED STRESS-OPTIC LAW

The optical properties of polymer solutions are associated with the polymer stress $\boldsymbol{\sigma}$ through a stress-optic law, and thus experimental measurements of birefringence can provide information on the polymer stress if the stress-optic law is known. The most common form of this law is a linear relation between the components of the index-of-refraction tensor and the corresponding components of the stress tensor—i.e., $n_{ij}=C\sigma_{ij}$ where C is the stress-optic coefficient [39,40]. For the problem of relaxation of initially straight polymers, no shear stress is developed in the system while the normal stress is dominated by the stress component σ_{11} where "1" is the direction of the initial extension (see Sec. III above). Since for this problem we have shown that the two independent refraction components n_{11} and n_{22} behave similarly to birefringence, we seek a stress-optic law as a relation between the polymer stress σ_{11} and the birefringence B. In addition, our goal is to provide a generalized law valid for any time and chain stiffness.

For the case of flexible chains, Doyle, Shaqfeh, and Gast [33] showed that the ratio of stress over the refraction component is constant at long times. In our notation, this law can be written as

$$\sigma_{11}/B = \text{const}. \tag{28}$$

The explanation of this simple relation lies in the fact that at long times $t \geq N^2$, the stress and optical properties show the same exponential decay resulting from the corresponding exponential decay of the polymer length. [See Figs. 4(a) and 7(b) in Ref. [37].]

In the recent work of Ghosh *et al.* [44], based on the similarities of the FENE and bead-rod models for flexible chains, a more general relation between stress and birefringence was found which in our notation can be written as

$$\sigma_{11} \sim \frac{NB}{B(0)-B}. \tag{29}$$

(The same relation was also proposed in the work of Doyle *et al.* [34] for the relaxation of several FENE-based models.) We note that this relation represents the relaxation of initially straight flexible chains and it is valid for intermediate and long times.

To derive a generalized stress-optic law valid for any time and stiffness we employ the specific mechanism via which the configuration relaxation affects the polymer stress and the chain's optical properties. In particular, in this paper we have established the relation between the chain's optical properties and the polymer length for both flexible and stiff chains

$$B(0) - B \approx [n_{11}(0) - n_{11}] + n_{22}$$

$$\sim \frac{1}{N}[R_{\parallel}^2(0) - R_{\parallel}^2] \sim \Delta R_{\parallel}, \tag{30}$$

where $\Delta R_{\parallel} \equiv R_{\parallel}(0) - R_{\parallel}$. We have also established the relation between the polymer stress and the chain's length for stiff chains:

$$\sigma_{11} \sim R_{\parallel} F_{\parallel} \sim N^2 \frac{d\Delta R_{\parallel}}{dt}, \tag{31}$$

where the dominant longitudinal tension forces are given by $F_{\parallel} \sim \zeta_{ch} d\Delta R_{\parallel}/dt$ while $\zeta_{ch} \sim N$ is the friction coefficient for the entire chain. Note that Eq. (31) is also valid for flexible chains as we discussed in our earlier work [37].

By combining Eqs. (30) and (31), a generalized stress-optic law is derived,

$$\sigma_{11} \sim N^2 \frac{d[B(0) - B(t)]}{dt}, \tag{32}$$

which is valid for both flexible and stiff chains, and for all time periods—i.e., for short, intermediate, and long times. One can easily verify analytically the universal validity of our stress-optic law by utilizing the known relaxation of stress and birefringence for both flexible and stiff chains at all time periods.

To show the validity of our stress-optic law numerically, in Fig. 8 we plot the ratio of the stress σ_{11} from our numerical results for flexible (from Ref. [37]) and stiff chains (presented in Sec. III) to the value predicted by our generalized stress-optic law, Eq. (32) above. Note that the increased noise results from the calculation of the derivative $d[B(0) - B(t)]/dt$ via a backward Euler time-integration scheme. This figure reveals that for any chain stiffness this ratio is approximately constant with time while for long chains it is ≈ 0.02; i.e., it is independent of the chain length N.

The generalized stress-optic law given by Eq. (32) reveals a nonlinear relationship between the polymer stress and the optical properties. We note that this nonlinearity results from the fact that the derivative $d[B(0) - B(t)]/dt$ is a nonlinear function of the birefringence B. For example, at the intermediate times of flexible chains and the early intermediate times of stiff chains, this law may result into the nonlinear Equation (29) above. During the late intermediate times of stiff chains, our stress-optic law may result in the following nonlinear equation:

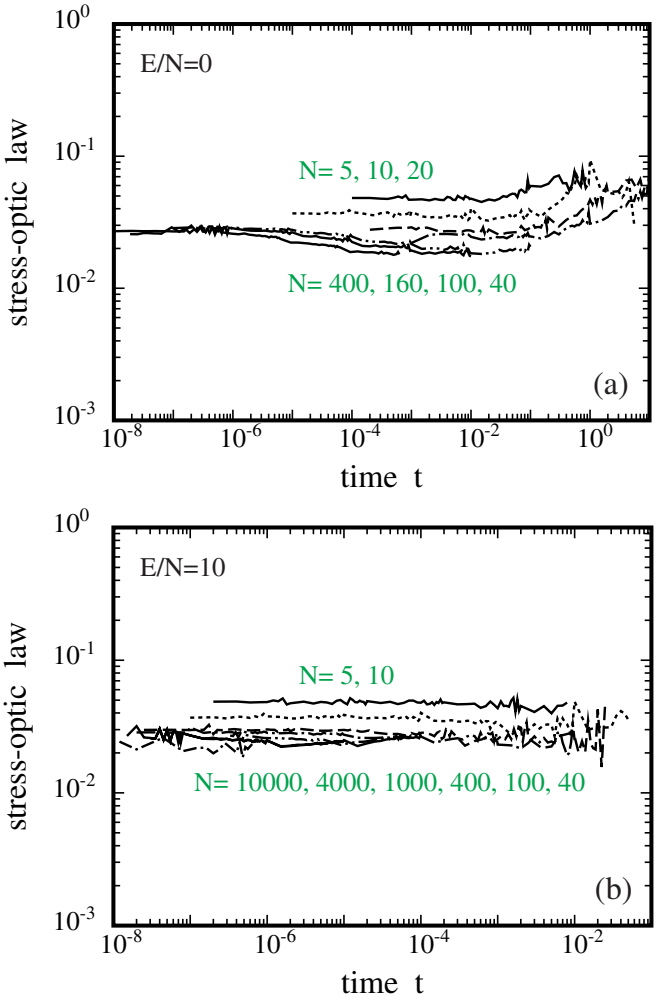

FIG. 8. (Color online) Generalized stress-optic law for flexible and stiff chains. (a) Completely flexible chains ($E=0$) with $N=5,10,20,40,100,160,400$. (b) Stiff chains ($E/N=10$) with $N=5,10,40,100,400,1000,4000,10000$. Note that we plot the ratio of σ_{11} from our numerical results (see Ref. [37] for flexible chains and Sec. III above for stiff chains) to the one predicted by Eq. (32). The increased noise results from the calculation of the derivative $d[B(0)-B(t)]/dt$.

$$\sigma_{11} \sim \left[\frac{(\Delta B)_{eq}}{B(0)-B}\right]^3, \tag{33}$$

where $(\Delta B)_{eq} \sim N^2/E$ is the scale of the birefringence reduction $B(0)-B$ at the end of the bending relaxation at times $\tau_\perp$ as we can deduce from Eq. (27) above.

VI. FORCE-EXTENSION RELATION

Physically the nonlinear stress-optic relationship results from the inherent nonlinearity of the current problem which is associated with the initial straight configuration of the polymer chain and produces a nonlinear force-extension relation. In particular, during the intermediate times of flexible chains and the early intermediate times of stiff chains, the longitudinal (tension) force is

$$F_\parallel \sim \zeta_{ch}\frac{d\Delta R_\parallel}{dt} \sim \frac{N}{\Delta R_\parallel} \sim \frac{N^2}{\Delta R_\parallel^2}, \tag{34}$$

while during the late intermediate times of stiff chains, this force is given by

$$F_\parallel \sim N^{-1}\left[\frac{(\Delta R_\parallel)_{eq}}{\Delta R_\parallel}\right]^3 \sim N^{-1}\left[\frac{(\Delta R_\parallel^2)_{eq}}{\Delta R_\parallel^2}\right]^3, \tag{35}$$

where $(\Delta R_\parallel^2)_{eq} \sim N^3/E$ is the scale of the length reduction $\Delta R_\parallel^2 \equiv R_\parallel^2(0) - R_\parallel^2$ at the end of the bending relaxation at times $\tau_\perp$. Only during the long times of flexible chains does Eq. (32) denote a linear stress-optic relationship [given by Eq. (28) above] since at these times both stress and birefringence are linear functions of the chain length [37] owing to the fact that the polymer chain is not far from equilibrium anymore, and thus the force-extension relation is linear.

The combination of Eqs. (34) and (35) along with a smooth transition at times τ_{mid} defines a new model for extended semiflexible bead road chains:

$$F_{\mathrm{ESBRC}} \sim \frac{N^2}{\Delta R_\parallel^2}\left[1+\left(\frac{\Delta R_\parallel^2}{N^3/E^{3/2}}\right)^2\right]^{-1}. \tag{36}$$

In the equation above F_{ESBRC} is the force along the chain's longitudinal direction while $N^3/E^{3/2}=(\Delta R_\parallel^2)_{mid}$ is the scale of the length reduction at the transition times τ_{mid}. For coarse-graining reasons, we may write Eq. (36) as

$$F_{\mathrm{ESBRC}} \sim \frac{L^2}{L^2-Q^2}\left[1+\left(\frac{L^2-Q^2}{L^3/L_p^{3/2}}\right)^2\right]^{-1}, \tag{37}$$

where Q is the chain's end-to-end distance. The numerical coefficient missing from Eq. (37) should be 1 if we want the ESBRC model to match the FENE model for flexible chains.

We emphasize that our ESBRC model is formally derived from the relaxation of an extended semiflexible polymer in the absence of external forces. However, one may use this model to describe the dynamics of a semiflexible polymer chain even under external forcing, the same way one may use the FENE model for flexible chains. (For example, one may consider a coarse-grain dumbbell chain where the spring force is given by the ESBRC model while the chain obeys the Langevin equation of motion.)

VII. DISCUSSION

In this section we address several issues that have arisen during the review process. Since these issues involve general questions on the computational model employed in our work and its association with recent analytical predictions, we think that it is for the reader's benefit to address these issues in a separate section which can be easily accessible for future reference.

In our work we utilize the semiflexible bead-rod model described in Sec. II. The same model has been employed by several research groups to study the dynamics of semiflexible polymers near and far from equilibrium—e.g., [23,26–28,38]. Results from this computational model show excellent agreement with analytical predictions based on the wormlike chain model; e.g., see [23,28].

The semiflexible bead-rod model we employ is based on the (flexible) bead-rod model developed by Grassia and Hinch [32] and includes a corrective potential force $\boldsymbol{F}_i^{cor}$ so that the equilibrium probability distribution of the chain configurations is Boltzmann as discussed in Sec. II. We emphasize that in our study the addition of these forces is a matter of preference; i.e., we obtain the same results even when these forces are omitted. (The inclusion of the corrective potential forces may affect the distribution of the angle between two successive links but it does not affect the bulk properties we study.)

In addition, the bead-rod model we employ is a discrete polymer model as commonly happens with other computational or even analytical polymer models. For any discrete model, the existence of a minimum length scale (e.g., the size of a bead or the link length) and the associated time scale (e.g., τ_{rand}) give rise to the so-called short-time behavior (e.g., the one discussed in Sec. III A). After this behavior, the polymer dynamics is independent of the model's discreteness. Because of this, some researchers prefer not to present the short-time behavior of their (computational or analytical) model; others prefer to present this behavior so that we are fully consistent with the model we employ. Most importantly, the short-time behavior reveals clearly the initial properties of the discrete chain (e.g., the tensions and polymer stress at full extension for the current problem) as well as the dynamics at the beginning of the intermediate-time behavior.

Another issue arising during the review process has to do with the $t^{7/8}$ scaling law (appearing in Ref. [23] and elsewhere) and the reason why this law does not appear in the present study. We emphasize that this law is valid in the linear regime of perturbations around equilibrium while in the current problem we study nonlinear perturbations. By employing (transient) Brownian dynamics simulations (as we do in our study) we can only investigate nonlinear dynamics. (Note that the linear dynamics are investigated computationally via correlations of fluctuations at equilibrium; e.g., see [23,26,27].) We emphasize that for the specific problem we study in this paper, the linear relaxation is already known from previous analytical and computational studies [23,26–28].

In addition, we emphasize that the results based on the relaxation of initially straight bead-rod chains (e.g., from the present work, our previous studies [37,38], and the study of Grassia and Hinch [32]) also represent the relaxation of extended bead-rod chains in strong flows after the flow is turned off. For example, Ref. [34] found a universal curve for relaxation after the cessation of strong flows which coincides with that for an initially straight flexible bead-rod chain. We also note that the bead-rod polymer model is always associated with finite tension forces even at full extension.

In the present work, we utilize the configuration relaxation and the associated mechanism we revealed in our recent Letter [38] to present and analyze the polymer properties including the polymer stress, the solution birefringence, and the configuration relaxation modes. In particular, our earlier study reveals that after the short-time (discrete) behavior, the polymer length shows an early $t^{1/2}$ universal relaxation (i.e., valid for any chain stiffness) and a late $t^{1/4}$ relaxation valid for semiflexible and stiff chains. In a later analytical study, Hallatschek, Frey, and Kroy [31] considered the longitudinal relaxation of stiff polymers in several external, linear and nonlinear, perturbations. For the relaxation of extended stiff polymers, the analytical study predicts the early $t^{1/2}$ and late $t^{1/4}$ power-law relaxation found in our earlier work [38]. (See Table II of the analytical work in [31].) In addition, Hallatschek, Frey, and Kroy predicted an intermediate $t^{1/3}$ power law due to homogeneous tension relaxation.

Thus, a question arises on the validity of this $t^{1/3}$ power law and, in general, the association between our earlier computational work [38] with the analytical study [31]. To address this issue, we should first discuss the limits of validity of the two types of studies. Our computations solve the full nonlinear Langevin equation (3) above; however, they are restricted to polymer chains with $E/N=10$ for the early relaxation (e.g., see Figs. 3 and 6). Our results for the late relaxation are much less restricted since in this paper we present results for $E/N=10$ and $E/N=10^4$ in Fig. 5.

On the other hand, analytical solutions may predict the chain evolution for a large stiffness range (e.g., for $E/N \gg 1$); however, due to the complexity (and nonlinearity) of the relevant problems, they may be based on unproved assumptions, while their range of validity is not well known. For example, the $t^{1/3}$ power law presented in Ref. [31] is predicted to be valid for $E/N \gg 1$; however, it is unclear what is the time duration of this law for the chains $E/N=10$ studied in our work.

Based on our computational results, currently we cannot verify or reject the analytical prediction of the intermediate $t^{1/3}$ power law. To explain this, observe that for any polymer property we have studied (e.g., length, width, stress, and birefringence), our computations reveal over many time decades the existence of the early and late behaviors. Between these two behaviors there exists a transition region of about one time decade; e.g., see Fig. 3. Due to its small size for chains with $E/N=10$, it is unclear if this region constitutes the predicted intermediate law or is just a transition from the early to the late behavior. To be able to verify or reject the intermediate $t^{1/3}$ power law computationally, one needs to study the early behavior (over extended time periods) of much stiffer chains which is currently unattainable.

Based on the same reasoning, currently one cannot verify or reject computationally not only this specific intermediate power law but even additional (analytically predicted) intermediate laws. However, one thing is certain: the earlier and later polymer behaviors should always be the $t^{1/2}$ and $t^{1/4}$ laws we found in our previous study [38]. (As explained in our Letter, at early times the chain stiffness cannot affect the longitudinal dynamics and thus the polymer should always show the universal $t^{1/2}$ law; the late $t^{1/4}$ law is well demonstrated by our numerical results for $E/N=10, 10^4$.) Thus, the existence of intermediate laws (if any) will not change our results discussed in this paper; they will merely change the transition time scale τ_{mid}. In addition, our reasoning of predicting and explaining the polymer properties will still be valid; e.g., the polymer stress during an intermediate behavior may be explained similarly to that for the early and late polymer stress presented in Sec. III above.

As a closure, we emphasize that although we discuss above the possibility of the existence of an additional intermediate power law, our own interpretation of our numerical results does not support this law. This can be easily understood based on our (low-noise) results for the polymer stress shown in Fig. 3(a) which reveal a rather rapid transition from the early to the late behavior.

VIII. CONCLUSIONS

In this paper we studied the relaxation of an initially straight stiff polymer by employing Brownian dynamics simulations based on a semiflexible bead-rod model. Our interest was concentrated on the stress and birefringence relaxation and how they are affected by the corresponding conformational relaxation of the polymer chain.

During the short times $t \ll \tau_{ten}$, the transverse free diffusion of the chain is not able to produce any stress relaxation and the birefringence shows a linear relaxation. During the early intermediate times $\tau_{ten} \ll t \ll \tau_{mid}$, the tension relaxation is associated with a length reduction $R_{\parallel}^2(0) - R_{\parallel}^2 \sim Nt^{1/2}$ and results in a strong-stress component relaxation of $\sigma_{11} \sim N^2 t^{-1/2}$ and a birefringence relaxation $B(0) - B \sim t^{1/2}$. Owing to the participation of the different relaxation modes in the transverse relaxation, the chain width increases anisotropically as $R_{\perp}^2 \sim N^{-1/3} t^{5/6}$ which produces a relaxation $\sigma_{22} \sim N^{2/3} t^{-1/6}$ for the weak-stress component. During the late intermediate times, the tension relaxation is associated with a length reduction $R_{\parallel}^2(0) - R_{\parallel}^2 \sim N^2 E^{-3/4} t^{1/4}$ and results in a strong-stress component relaxation of $\sigma_{11} \sim N^3 E^{-3/4} t^{-3/4}$ and a birefringence relaxation $B(0) - B \sim NE^{-3/4} t^{1/4}$. The transverse relaxation modes result in an anisotropical width increase $R_{\perp}^2 \sim E^{-1/4} t^{3/4}$ and a weak-stress component relaxation of $\sigma_{22} \sim NE^{-1/4} t^{-1/4}$.

It may prove useful to future studies to determine the numerical coefficient of the time scales appearing in this article. Figure 2 shows that $\tau_{bend} \approx 10^{-3} E^{-1}$ while $\tau_{ten} \approx 10^{-2} N^{-2}$ based on Fig. 1. In addition, Fig. 4 shows that $\tau_{\perp} \approx 10^{-3} N^4 / E$. (Note that τ_{bend} and $\tau_{\perp}$ should have the same numerical coefficient since they belong to the same series of time scales.) Figure 3 suggests that $\tau_{mid} \approx 10^{-5} N^4 / E^3$. Based on the property of the scaling law methodology which dictates that the behavior of short chains represent the late behavior of longer chains [43], the same coefficient is derived if we require that $\tau_{ten} \approx \tau_{mid}$ and assume that this occurs for $N \approx 10(E/N)$. We emphasize that all these numerical coefficients are approximate estimates since the transition from one to the next behavior does not occur at an exact time but occupies a time zone.

The longitudinal relaxation of the polymer chain at the early intermediate times constitutes a universal behavior valid for any stiffness of the bead-rod chain. The same happens for any polymer property which depends only on the chain length such as the strong stress component σ_{11} and the chain's optical properties (i.e., the birefringence and the refraction components). On the other hand, during the late intermediate times, both the longitudinal and transverse relaxations of the polymer chain (and thus all the polymer properties which depend on the chain's length or width) were shown to be valid for any stiff chain $E \geq N$.

By combining the relation between the optical properties and the chain configuration with the relation between the polymer stress and the chain configuration, we proposed a generalized stress-optic law describing the relaxation for any chain stiffness and time period. We emphasize that the inherent nonlinearity of the current problem (associated with the initial straightness of the polymer chain) results in a nonlinear force-extension relation and the nonlinear stress-optic law given by Eq. (32). A coarse-grain model describing extended semiflexible bead road chains (ESBRC) was also proposed.

Knowledge of the physical mechanism and the chain's conformational behavior helps us understand the properties of the polymer solution. In this paper by employing this procedure, we were able to predict and explain the polymer stress and optical relaxation. It is important to realize that the (bulk) properties of the polymer solution—e.g., stress and birefringence—are functions of the chain configuration and thus can be predicted and explained based on the knowledge of the conformational behavior. Therefore, we believe that the methodology we employ in this article is well suited to study other problems in the area of polymer dynamics.

ACKNOWLEDGMENTS

This work was supported by the Minta Martin Research Fund at the University of Maryland. The computations were performed on multiprocessor computers provided by the National Center for Supercomputing Applications in Illinois (Grant No. DMR000003) and by an Academic Equipment Grant from Sun Microsystems Inc.

[1] T. T. Perkins, S. R. Quake, D. E. Smith, and S. Chu, Science **264**, 822 (1994).
[2] T. T. Perkins, D. E. Smith, and S. Chu, in *Flexible Polymer Chains in Elongational Flow*, edited by T. Q. Nguyen and H-H Kausch (Springer, Berlin, 1999).
[3] G. J. L. Wuite, S. B. Smith, M. Young, D. Keller, and C. Bustamante, Nature (London) **404**, 103 (2000).
[4] T. B. Liverpool, R. Golestanian, and K. Kremer, Phys. Rev. Lett. **80**, 405 (1998).
[5] D. J. Bicout and R. J. Rubin, Phys. Rev. E **59**, 913 (1999).
[6] B. Schnurr, F. Gittes, F. C. MacKintosh, and C. F. Schmidt, Macromolecules **30**, 7781 (1997).
[7] F. Gittes, B. Schnurr, P. D. Olmsted, F. C. MacKintosh, and C. F. Schmidt, Phys. Rev. Lett. **79**, 3286 (1997).
[8] J. Y. Xu, A. Palmer, and D. Wirtz, Macromolecules **31**, 6486 (1998).
[9] T. Gisler and D. A. Weitz, Phys. Rev. Lett. **82**, 1606 (1999).
[10] T. G. Mason, T. Gisler, K. Kroy, E. Frey, and D. A. Weitz, J.

Rheol. **44**, 917 (2000).
[11] Y. Tseng, B. W. Schafer, S. C. Almo, and D. Wirtz, J. Biol. Chem. **277**, 25609 (2002).
[12] A. Caspi, M. Elbaum, R. Granek, A. Lachish, and D. Zbaida, Phys. Rev. Lett. **80**, 1106 (1998).
[13] M. Milas, I. Roure, and G. C. Berry, J. Rheol. **40**, 1155 (1996).
[14] A. R. Evans and E. S. G. Shaqfeh, J. Non-Newtonian Fluid Mech. **64**, 95 (1996).
[15] R. Diaz-Calleja, M. J. Sanchis, C. Alvarez, and E. Riande, J. Appl. Phys. **81**, 3685 (1997).
[16] G. C. Berry, Macromolecules **32**, 7939 (1999).
[17] R. G. Larson, T. T. Perkins, D. E. Smith, and S. Chu, Phys. Rev. E **55**, 1794 (1997).
[18] C. M. Schroeder, H. P. Babcock, E. S. G. Shaqfeh, and S. Chu, Science **301**, 1515 (2003).
[19] J. Käs, H. Strey, M. Bärmann, and E. Sackmann, Europhys. Lett. **21**, 865 (1993).
[20] J. Käs, H. Strey, J. X. Tang, D. Finger, R. Ezzell, E. Sackmann, and P. A. Janmey, Biophys. J. **70**, 609 (1996).
[21] D. Riveline, C. H. Wiggins, R. E. Goldstein, and A. Ott, Phys. Rev. E **56**, R1330 (1997).
[22] R. Granek, J. Phys. II **7**, 1761 (1997).
[23] R. Everaers, F. Julicher, A. Ajdari, and A. C. Maggs, Phys. Rev. Lett. **82**, 3717 (1999).
[24] F. Gittes and F. C. MacKintosh, Phys. Rev. E **58**, R1241 (1998).
[25] D. C. Morse, Phys. Rev. E **58**, R1237 (1998).
[26] M. Pasquali, V. Shankar, and D. C. Morse, Phys. Rev. E **64**, 020802 (2001).
[27] P. Dimitrakopoulos, J. F. Brady, and Z.-G. Wang, Phys. Rev. E **64**, 050803(R) (2001).
[28] V. Shankar, M. Pasquali, and D. C. Morse, J. Rheol. **46**, 1111 (2002).
[29] U. Seifert, W. Wintz, and P. Nelson, Phys. Rev. Lett. **77**, 5389 (1996).
[30] P. Ranjith and P. B. S. Kumar, Physica A **318**, 220 (2003).
[31] O. Hallatschek, E. Frey, and K. Kroy, Phys. Rev. Lett. **94**, 077804 (2005).
[32] P. S. Grassia and E. J. Hinch, J. Fluid Mech. **308**, 255 (1996).
[33] P. S. Doyle, E. S. G. Shaqfeh, and A. P. Gast, J. Fluid Mech. **334**, 251 (1997).
[34] P. S. Doyle, E. S. G. Shaqfeh, G. H. McKinley, and S. H. Spiegelberg, J. Non-Newtonian Fluid Mech. **76**, 79 (1998).
[35] E. S. G. Shaqfeh, G. H. McKinley, N. Woo, D. A. Nguyen, and T. Sridhar, J. Rheol. **48**, 209 (2004).
[36] C. M. Schroeder, E. S. G. Shaqfeh, and S. Chu, Macromolecules **37**, 9242 (2004).
[37] P. Dimitrakopoulos, J. Fluid Mech. **513**, 265 (2004).
[38] P. Dimitrakopoulos, Phys. Rev. Lett. **93**, 217801 (2004).
[39] G. G. Fuller, Annu. Rev. Fluid Mech. **22**, 387 (1990).
[40] R. G. Larson, *The Structure and Rheology of Complex Fluids* (Oxford University Press, Oxford, 1999).
[41] M. Doi and S. F. Edwards, *The Theory of Polymer Dynamics* (Clarendon, Oxford, 1986).
[42] H. Yamakawa, *Helical Wormlike Chains in Polymer Solutions* (Springer, Berlin, 1997).
[43] P. Dimitrakopoulos, J. Chem. Phys. **119**, 8189 (2003).
[44] I. Ghosh, G. H. McKinley, R. A. Brown, and R. C. Armstrong, J. Rheol. **45**, 721 (2001).